Voltage Unbalance Correction in a Grid Using Inverter

K.Jayakumar[1], N.Sriharish[2], Ch.Rambabu[3]

1 M.Tech Student in Power Electronics, Dept. of EEE at Sri Vasavi Engineering College, Tadepalligudem, A.P, India
2 Assistant Professor, Dept. of EEE at Sri Vasavi Engineering College, Tadepalligudem, A.P, India
3 Professor & HOD, Dept. of EEE at Sri Vasavi Engineering College, Tadepalligudem, A.P, India

Abstract

This paper presents the control of a "voltage unbalance correction in a grid using inverter". The inverters are proposed give additional function to decrease the negative sequence voltage at the point of correction with the utility grid. By using improved multi variable filter, the grid inverter absorbs a small amount of negative sequence current from the grid, and which based up on symmetric sequence voltage decomposition, thereby helping to correct the negative sequence voltage. But the amplitude reduction by each individual inverter system is small as compared to the entire negative sequence component, and these inverter modules can achieve to collect substantial results in the grid. Finally the analyses of the scheme along with the suitable design are presented by using basic circuit diagram and proposed control has been verified by simulation results are shown.

Keywords: PWM inverter, multi variable filter, voltage unbalance, point of correction, negative sequence voltage, distributed generation, grid interfacing etc.

I. Introduction:

In practical three phase power systems, voltage unbalance problems are existing. These problems are mainly caused by single phase and non-linear loads, which are unequally distributed. Therefore these unequal voltage drops are mainly occur across transformers and line impedances. Here the negative sequence voltages are especially troublesome in practical applications. Due to this the zero sequence component are not exist in three wire systems. These voltage unbalance effect is quite serve for electrical machines, power electronic converters and its drives [1]. So to mitigate this voltage unbalance we can go to design power electronic converters for regulating the reactive power [2, 3]. But in underground cables this approach is not suitable because in underground cables the resistance of the cable dominates its inductance. To maintain a balanced voltage at the load terminals, an often used idea is to inject a series voltage [4, 5]. It is straightforward to mitigate the voltage unbalance problem with such converters, but a disadvantage is that they are unused or only lightly loaded when there are no voltage unbalance problems. For dealing with other power quality problems than voltage unbalance, so-called unified power quality conditioners (UPQC) are proposed and continuously improved. However, the UPQC has no energy storage capabilities [6], and should be extended to cope with distributed generation (DG) [7].

Facing the emerging application of distributed generation, power electronics-based grid-interfacing inverters are playing an important role interfacing DGs to the utility grid. In addition to conventional delivery of electricity, ancillary functionality for improvement of power quality problems is being introduced into grid-interfacing inverters [8, 9]. In this paper, it is proposed to integrate voltage unbalance correction into the control of grid-interfacing inverters. This does not require more hardware, since the feedback variables for this control are already available. By controlling the negative-sequence currents, which induce opposite negative-sequence voltage drops on the line impedances, the objective of eliminating negative sequence voltages at the point of connection (PoC) with the grid may be achieved. To investigate the effectiveness of the proposed function, a three-phase four-wire inverter is used to control voltage unbalance correction. The employed inverter operates normally when the utility voltages are balanced, and when unbalanced, performs compensation automatically for negative-sequence voltage, based on utility voltage unbalance factor (VUF) [1]. To this aim, the analysis of negative-sequence current control and high performance detection for symmetrical sequences are introduced in the following. Then, the inverter control scheme and reference signal generation are presented. Finally, the proposed control methods are verified by simulations.

II. Grid-interfacing inverter with integrated voltage unbalance correction:

Fig. (1) shows the structure of a three-phase four-wire grid-interfacing system being connected to the utility grid at the POC through LCL filters. It normally synchronizes with the utility grid and delivers electrical energy to the grid from the DC-bus when pre-regulated distributed sources are connected. The voltage unbalance correction function is added, which intentionally regulates negative sequence currents. Note that, in order to obtain a maximum power factor, most grid-interfacing inverters deliver only positive-sequence currents under either balanced or unbalanced conditions. Therefore, the development of this proposed controller differs from the conventional one, and its design will be presented in the next sections of this paper. In

view of unbalanced situations, a four-leg inverter topology is used as the circuit to eliminate zero-sequence currents. With the theory of symmetric decomposition for three phase systems [10], unbalanced grid voltages can be divided into three groups, namely positive, negative, and zero sequence voltages. Similarly, current quantities can also be separated. By disregarding the mutual coupling between the grid lines in Fig. (1), an equivalent circuit model for each group of sequence components can be derived [11]. The diagram for negative-sequence components is shown in Fig.(2), where the superscript "-" denotes negative sequence. Similarly, the superscript "+" denotes positive sequence. Phasors V_g^- and V_s^- are the negative-sequence voltages of the utility grid and at the PoC, respectively. Current I_s^- is the negative-sequence current equivalent line impedance is represented by Zg, the equivalent impedance of the utility grid when the line impedances of the three phases are assumed symmetrical.

Accordingly, a phasor diagram showing the change for negative-sequence fundamental current is drawn in Fig.(3). By changing the amplitude and phase of the negative sequence current I_s^-, the negative-sequence voltage V_s^- can be regulated through the voltage drops across the line impedance. For a given amplitude I_s^-, the voltage changes along the dashed circle and reaches a minimum value at the point M where θ^- equals the negative of impedance angle of Zg's. Similarly, zero-sequence voltages at the PoC can be compensated by regulating the zero-sequence currents within the system. This paper only concentrates on the correction of negative-sequence voltages, considering zero-sequence voltages do not exist in case of three wire systems. Of course, zero-sequence voltages can be isolated by transformers when needed. Furthermore, it is noted that measurements of zero-sequence components can be done simply by adding three phase while accurate positive- and negative-sequence components are difficult to be determined. Therefore, zero sequence voltage correction can be trivially added to the control based on the proposed control scheme for negative-sequence voltage correction and is not discussed in this paper.
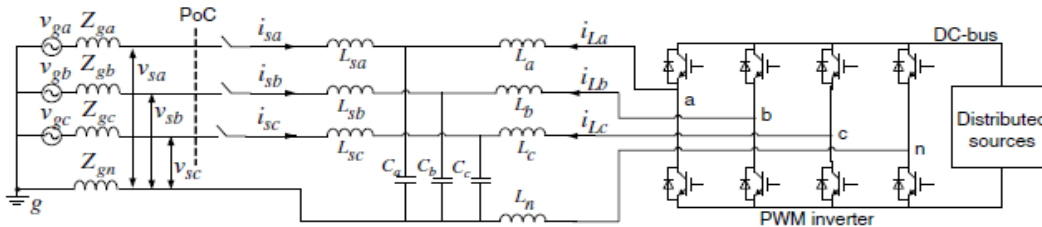

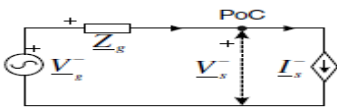Fig.(1) Three-phase four-wire grid-interfacing four leg inverter at PoC.
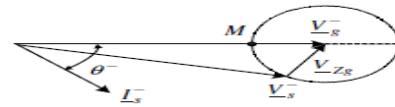

Fig.(2) Negative-sequence equivalent model   Fig.(3) Phasor diagram of the negative-sequence model.

III. Control scheme:

A. Determination of Negative-sequence Currents

Fig. (3) Illustrates the basic principle of how to correct unbalanced voltage at the PoC with sequence-current control. It is suggested to determine the negative-sequence currents based on the voltage unbalance factor. To assess unbalanced voltages at the PoC, the voltage unbalance factor, *KVUF* is defined as the ratio between the amplitude of the negative-sequence voltage V_s^- and the amplitude of the positive-sequence voltage V_s^+. The following constraint equation is proposed to calculate the desired current amplitude I_s^-:

$$\frac{I_s^-}{I_s^+} = \frac{V_s^-}{V_s^+} = K_{VUF},\qquad(1)$$

where I_s^+ is the amplitude of the positive-sequence current. Then, the resulting I_s^- is derived based on the ratio of unbalance voltages at the PoC from (1).

However, the voltage unbalance factor at the PoC varies with the controlled negative-sequence currents, because the controller utilizes feed forward measurements of K_{VUF} and operates in a open-loop. Consequently, this strategy may cause the value of K_{VUF} in (1) to vary. To ensure a stable correction, a smooth update method for K_{VUF} is added to the control. The flow chart shown in Fig.(4) illustrates how to derive the final I_s^-. The currently measured quantity is referred to as $K_{VUF}(n)$, and the

previous one is $K_{VUF}(n-1)$. In Fig.(4), the minimum threshold (*Kmin*) of negative-sequence correction is defined according to practical demands, and a coefficient denoted by λ is introduced for smooth regulation when decreasing the output value of K_{VUF}. Note that, for system protection, the current rating of the inverters is always checked before returning I_s^-.
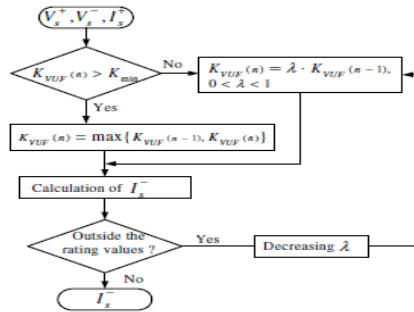

Fig.(4) Flow chart of K_{VUF} determination.

B. Positive- and Negative-Sequence Detection

The factor K_{VUF} is essential to get the amplitude of negative-sequence currents. Thus the separation of sequence voltages is central to get the value of K_{VUF}, as well as to the synchronization with the utility grid. For unbalanced or distorted grid voltages, a multi-variable filter was introduced in [12] for detecting the positive-sequence component in the stationary frame. After modification, this filter is able to directly filter out the fundamental positive and negative-sequence vectors. The following mathematically demonstrates the multi- variable filter for symmetric sequence decomposition.

For unbalanced distorted voltages, the positive- and negative-sequence components are in the $\alpha - \beta$ frame as expressed by

$$v_{\alpha\beta}(t) = v_\alpha(t) + jv_\beta(t)$$

$$= \sum_{k=1}^\infty (V_k^+ e^{jk\omega_1 t} + V_k^{o-} e^{-jk\omega_1 t}) \qquad (2)$$

where k denotes the harmonic number, $\omega 1$ denotes the fundamental radian frequency, and the superscript symbol "o" denotes conjugate.

Let us look for a filter $G^+(t)$, which can damp all harmonic components of $v_{\alpha\beta}(t)$ but the fundamental positive –sequence component in the stationary frame. That is,

$$v_{\alpha\beta}(t) * G^+(t) = v'_{\alpha\beta}(t), \qquad (3)$$

where the "*" denotes a convolution product, and

$$v'_{\alpha\beta}(t) = V_1^+ e^{jk\omega_1 t} + \sum_{k=3,5...}^\infty U_k^+ e^{jk\omega_1 t} + \sum_{k=1,3...}^\infty U_k^{o-} e^{-jk\omega_1 t} \qquad (4)$$

with $\| U_k^+ \| \ll \| V_1^+ \|$ and $\| U_k^{o-} \| \ll \| V_1^- \|$.

Otherwise stated $v'_{\alpha\beta}(t) \approx v^+{}_{\alpha\beta}(t) = V_1^+ e^{j\omega_1 t}$ the fundamental positive-sequence component of $v_{\alpha\beta}(t)$ as defined in (2).

By multiplying $v_{\alpha\beta}(t)$ and $v'_{\alpha\beta}(t)$ with $e^{-j\omega_1 t}$, respectively, which corresponds to a transformation to a positive synchronous rotating frame (PSRF), we obtain from (2) and (3)

$$v_{\alpha\beta}(t) e^{-j\omega t} = V_1^+ \sum_{k=2,4...}^\infty (V_k^+ e^{jk\omega_1 t} + V_k^{o-} e^{-jk\omega_1 t}),$$

$$v'_{\alpha\beta}(t) e^{-j\omega_1 t} = V_1^+ e^{jk\omega_1 t} + \sum_{k=2,4...}^\infty (U_k^+ e^{jk\omega_1 t} + U_k^{o-} e^{-jk\omega_1 t}) \qquad (5)$$

It can be seen that the fundamental positive-sequence voltage performs as a DC quantity in the PSRF. Therefore, a simple first order filter $H(t)$ with

$$L[H(t)] = H(s) = \frac{\omega_b}{s + \omega_b} \tag{6}$$

where ω_b is the corner frequency, is sufficient to get $v'_{\alpha\beta}(t)e^{-j\omega_1 t}$ from $v_{\alpha\beta}(t)e^{-j\omega_1 t}$ under the conditions of (4). This can be expressed with

$$v_{\alpha\beta}(t)\, e^{-j\omega_1 t} * H(t) = v'_{\alpha\beta}(t)\, e^{-j\omega_1 t} \tag{7}$$

or, using Laplace

$$v_{\alpha\beta}(s + j\omega_1)H(s) = v'_{\alpha\beta}(s + j\omega_1) \tag{8}$$

Substituting $s \leftarrow s - j\omega_1$ into (6) and (8), it follows that

$$v_{\alpha\beta}(s).\frac{\omega_b}{s - j\omega_1 + \omega_b} = v'_{\alpha\beta}(s) \tag{9}$$

From (3), we also have

$$v_{\alpha\beta}(s)G^+(s) = v'_{\alpha\beta}(s) \tag{10}$$

Therefore, $G^+(s)$ the filter we are looking for, in the stationary frame should be equal to

$$G^+(s) = H(s - j\omega_1) = \frac{\omega_b}{s - j\omega_1 + \omega_b} \tag{11}$$

By expanding (10) to

$$v'_\alpha(s) + jv'_\beta(s) = \frac{\omega_b}{s - j\omega_1 + \omega_b}[v_\alpha(s) + jv_\beta(s)] \tag{12}$$

the following equations are derived

$$v'_\alpha(s) = \frac{1}{s}[\omega_b\left(v_\alpha(s) - v'_\alpha(s)\right) - \omega_1 v'_\beta(s)]$$

$$v'_\beta(s) = \frac{1}{s}[\omega_b\left(v_\beta(s) - v'_\beta(s)\right) - \omega_1 v'_\alpha(s)] \tag{13}$$

Similarly, the fundamental negative-sequence component follows as

$$v_{\alpha\beta}(t) * G^-(t) = v''_{\alpha\beta}(t) \tag{14}$$

Where, $v''_{\alpha\beta}(t) = V_1^{o+} e^{-j\omega_1 t} + \sum_{k=1,3...}^{\infty} U_k^+ e^{jk\omega_1 t} + \sum_{k=3,5...}^{\infty} U_k^{o-} e^{-jk\omega_1 t}$ $\tag{15}$

Or $v''_{\alpha\beta}(t) \approx v^-_{\alpha\beta1}(t)$ similar to (8) and (10), we have

$$v_{\alpha\beta}(s - j\omega_1).H(s) = v''_{\alpha\beta}(s - j\omega_1)$$

$$v_{\alpha\beta}(s).G^-(s) = v''_{\alpha\beta}(s) \tag{16}$$

Where, $G^-(s) = \frac{\omega_b}{s + j\omega_1 + \omega_b}$

Correspondingly, the equations below are derived:

$$v_\alpha''(s) = \frac{1}{s}[\omega_b(v_\alpha(s) - v_\alpha''(s)) - \omega_1 v_\beta''(s)]$$

$$v_\beta''(s) = \frac{1}{s}[\omega_b(v_\beta(s) - v_\beta''(s)) - \omega_1 v_\alpha''(s)] \qquad (17)$$

Therefore, the detection for $v_{\alpha 1}^+(t) + j v_{\beta 1}^+(t)$ and $v_{\alpha 1}^-(t) - j v_{\beta 1}^-(t)$ are approximately achieved from (13) and (17). These equations can be easily implemented in the $\alpha - \beta$ frame by digital control, without complicated transformation to the SRF and the inverse transformation.

In practical applications, the negative-sequence component is too small to be detected accurately. This is because the input signals involve a large proportion of positive sequence components which are difficult to damp totally. Alternative signals $\hat{v}_{\alpha\beta}(t)$, with

$$\hat{v}_{\alpha\beta}(t) = \hat{v}_\alpha(t) + j\hat{v}_\beta(t) = v_{\alpha\beta}(t) - v^+{}_{\alpha\beta 1}(t) \qquad (18)$$

where the dominant positive-sequence component $v^+{}_{\alpha\beta 1}(t) = v_{\alpha 1}^+(t) + jv_{\beta 1}^+(t)$ is abstracted, and can be used as input signals. This will improve the filtering effect for negative-sequence quantities.

Fig. (5) illustrates the implementation diagram of the multiple-variable filter, where the bandwidth ω_b for the positive- and negative-sequence filter is denoted by ω_{b1} and ω_{b2} respectively (the values can be different and adapted to practical situations). The central frequency ω_1 is set at the fundamental frequency of the grid voltage. In case of grid frequency variations the bandwidth can be increased slightly, or ω_1 can be adaptively updated with the measured fundamental frequency.
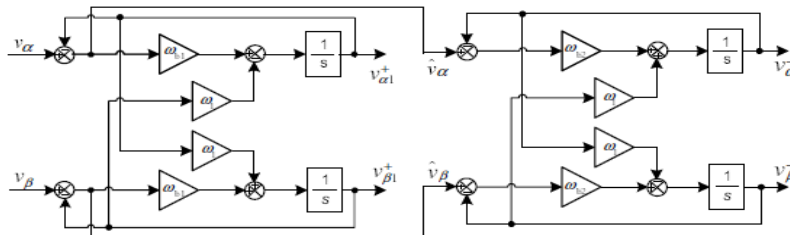

Fig. (5) Implementation diagram of the multi-variable filter

A frequency domain multi-variable filter plot is drawn in Fig. 6, based on (10) and the second equation in (16). Due to unity gain and zero phase-shift of the positive - sequence filter at the central frequency (50Hz), $\hat{v}_\alpha(t) + j\hat{v}_\beta(t)$ can be directly derived, see Fig. (5).

C. Reference signals generation

Fig. (6) shows the block diagram of the inverter's current reference generator. It consists of the detection of symmetric sequence voltages with a multi-variable filter, the VUF calculation, average power regulation and the signal synthesis. The first two processes have been detailed in the previous two subsections. By utilizing the fundamental positive - and negative-sequence components filtered out by the filter, we can obtain

$$V_{mag}^+ = \sqrt{v_{\alpha 1}^{+2} + v_{\beta 1}^{+2}}$$

$$V_{mag}^- = \sqrt{v_{\alpha 1}^{-2} + v_{\beta 1}^{-2}} \qquad (19)$$

where V_{mag}^+ and V_{mag}^- denote the magnitude of fundamental positive- and negative-sequence voltage, respectively.

Consequently, two groups of per-unit signals can be derived with divisions, that is as shown in Fig. (6). According to the principle described in section II, negative-sequence currents are designed to keep a phase-shift $\theta-$ with the negative-sequence voltage. This phase-shift equals the negative line impedance angle for the maximum correction effect. Its mathematical derivation is

$$i_{s\alpha}^- * + j i_{s\beta}^- * = (i_\alpha^- * + j i_\beta^- *) e^{j\theta^-} \tag{20}$$

The positive-sequence current references are either inphase or in anti-phase with the positive-sequence component of the grid voltage, depending on the desired direction for energy delivery. In this paper, the gain K_{dir} is set -1 in order to deliver energy to the utility grid. In the average power control loop of Fig.(6), the power reference P^* is given, which can be determined according to the application, such as the active power generated by upstream DG or the power demanded by the downstream utility grid. In order to eliminate the effects of double fundamental frequency ripple on the measured average power, the parameters should have a small proportional gain and a big integration time constant. In this work, the gain is chosen as 0.04 and the time constant is 0.02s. The output of the PI controller is used to regulate the amplitudes of the desired currents with the coefficient K_c.

All together, it follows that the current references $i_{s\alpha}^*$ and $i_{s\beta}^*$ are derived in the stationary frame. This is beneficial for the controller design, since the controller presented in the next section is also designed in the stationary frame. The mathematical manipulations to optimally implement the above digital process are not the subject of this paper, and will be discussed elsewhere.
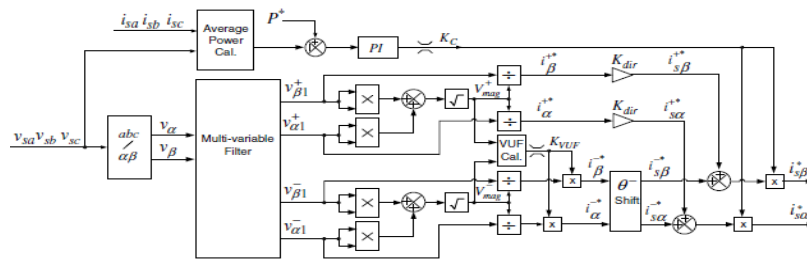

Fig. (6) Current reference generation for the inverter control.

D. Controller for Current Regulation

Fig. (7) shows the controller structure of the grid interfacing inverter. It is constructed by a double-loop current controller, which is an outer control loop with proportional-resonant (PR) controllers for eliminating the zero steady-state error of the delivered currents, and an inner capacitor current control loop with simple proportional controllers to improve stability. Instead of direct sampling, capacitor currents are calculated from the output currents and the inner filter inductor currents. These currents are measured anyway for over-current protection. To eliminate the zero-sequence currents in unbalanced situations, the current reference $i_{s\gamma}^*$ should be zero. The control for both positive- and negative-sequence components would be much too complicated and computation-time consuming when conventional PI control with coordinate transformation were used. Therefore, it is preferred to choose a PR controller in the stationary frame. A quasi-proportional-resonant controller with high gain at the fundamental frequency is used,

$$G_i(s) = K_p + \frac{2K_r \omega_{br} s}{s^2 + 2\omega_{br} s + \omega_1^2} \tag{21}$$

Where K_p are the proportional gain, K_r the resonant gain, and ω_{br} the equivalent bandwidth of the resonant controller. A detailed design for the PR controller has been presented in [13], it is not duplicated here. Through optimizing, the parameters used in the simulation are K_p =0.5, K_r =50, and ω_{br} =20.

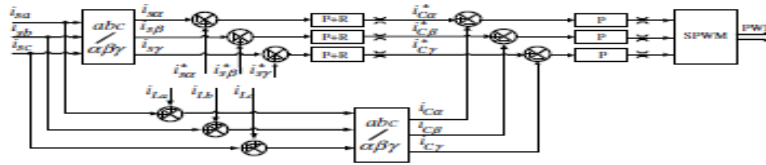Fig. (7). Structure of the controller for current regulation
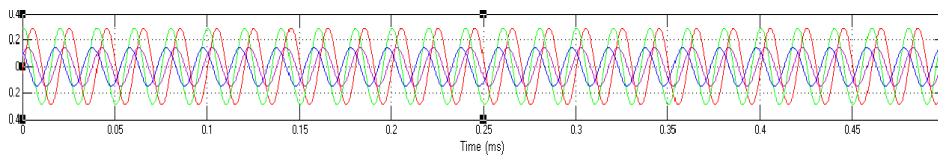
VI. Simulation Results:

Simulation results from mat lab / simulink are provided to enable the verification of the reference signals generation. The system parameters are shown in the below table. In order to easily observe the effects of negative-sequence correction, we intentionally blown-up the values of the line inductances to the same order as the filter inductors. Therefore, the inductors L_{sa}, L_{sb}, L_{sc} are combined with the line impedances, reducing the LCL structure to an LC one. According to the values of the line impedances in below, we obtain that $\theta = 45$ degrees. For a straightforward test of the effectiveness caused by the negative-sequence voltage correction, only fundamental positive- and negative-sequence components are considered in the grid voltages as given. It should be pointed out that the afore-mentioned control scheme and the multi-variable filter can also be implemented for distorted grid voltages.
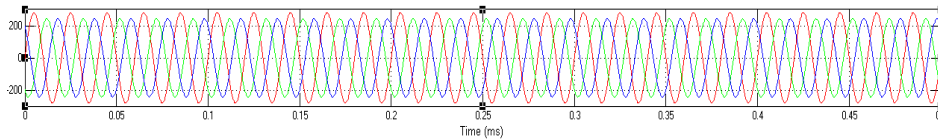
(a) unbalanced grid voltages in a-b-c frame
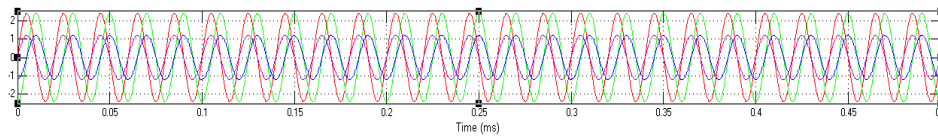
(b) per-unit positive sequence currents $i_{s\alpha}^{+*}$ and $i_{s\beta}^{+*}$ in-phase with the positive-sequence voltage

(c) negative-sequence current $i_{s\alpha}^{-*}$ and $i_{s\beta}^{-*}$ lags the negative-sequence voltage by 45 *degrees* in the $\alpha - \beta$ frame.

Fig. (8). Simulation results of the reference currents generation.

To verify the proposed control method with its integrated correction function, the controller is designed on a Mat lab Simulink. Due to the long computation time of the controller, a sampling frequency of 8 kHz is used. The switching frequency is twice the sampling frequency.

From the above fig.(8) shows the simulation results of reference current generation. And this simulation wave form shows the (a). Unbalanced grid voltages in a-b-c frame, (b).per-unit positive sequence currents $i_{s\alpha}^{+*}$ and $i_{s\beta}^{+*}$ in-phase with the positive-sequence voltage, (c).negative-sequence current $i_{s\alpha}^{-*}$ and $i_{s\beta}^{-*}$ lags the negative-sequence voltage by 45 *degrees* in $\alpha - \beta$ frame.

Fig. (9). show the simulation waveforms of the Grid-interfacing inverter with integrated negative-sequence voltage correction. The plots are the unbalanced grid voltages, the controlled line currents, and the voltages at the PoC, respectively. Using unbalanced grid voltages, the inverter delivers mainly positive-sequence currents to the utility grid and absorbs 10% of the negative-sequence currents. The effectiveness of the multi-variable filter in detecting positive- and negative-sequence

components from unbalanced voltages is shown in Fig.(10). For observing, these simulation waveforms of The RMS value and phase-shift of the positive- and negative-sequence voltages show almost the same results as the calculation results from $a - b - c$ quantities to $\alpha - \beta$ quantities. To observe the negative-sequence voltage correction, the results are illustrated in $\alpha - \beta$ frame by decomposing voltages from the $a-b-c$ frame. As seen in Fig.(11), the amplitude of the negative-sequence voltage at the PoC is reduced, although the decrease is limited to around 10%. Again note that the line impedance parameters have been blown up. In a utility grid, for instance $200\mu H$ line impedance is more realistic, and then the decrease would be around 1% for the same conditions. However, based on multiple modules, the effect of the negative-sequence voltage correction will be more pronounced.

Qualitatively, we can assume that the regulated negative sequence currents by the modules in Fig.(12) can be lumped into a single module, and therefore should behave identical to the single inverter and its results are shown in Fig.(11). And fig.(13) shows the corrected voltage at the PoC when we simply provide more negative-sequence current. It can be seen that the three-phase voltages tend to be balanced. This generally indicates the effectiveness of distributed voltage unbalance correction. However, it must be noted that the proposed method is only an alternative. It is preferable in an unbalanced situation with small voltage deviation, while the conventional methods are suitable for serious situations with large voltage unbalance.
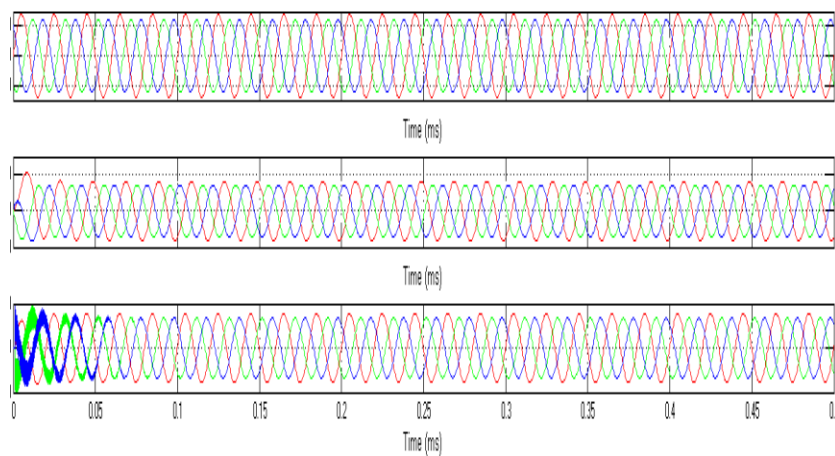

Fig.(9). Simulation results of the grid-interfacing inverter with integrated voltage unbalance correction

(a) Unbalanced grid voltages, (b) Currents delivered by the inverter, (c) Voltages at the PoC.
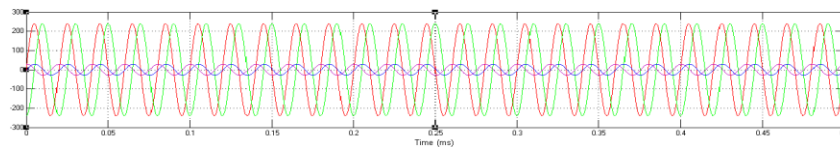

Fig. (10). Simulation waveforms of positive- and negative-sequence voltage detection, where the filtered out fundamental symmetric sequence voltages are derived in $\alpha - \beta$ frame.
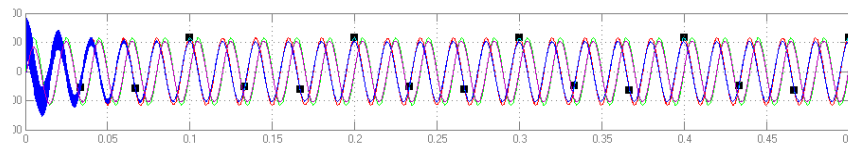

Fig. (11). Simulation results of the negative-sequence voltage correction. The α, β components of the negative-sequence voltage of the PoC $v_{s\alpha}^-$, $v_{s\beta}^-$ shows a 10% amplitude reduction compared with the negative sequence voltage of the grid $v_{g\alpha}^-$, $v_{g\beta}^-$.
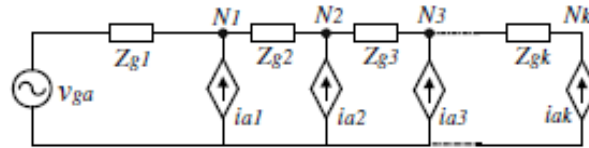
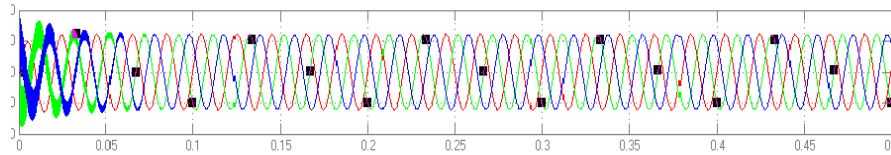Fig.(12). Per-phase equivalent circuit with multiple modules.

Fig.(13). Simulation waveforms of the negative-sequence voltage correction. The resulting corrected voltages tend to be balanced.

V. System Parameters:

DESCRIPTION	SYMBOL	VALUE
Grid voltage	V_{ga}	198V∟0°
	V_{gb}	171.71V∟125.21°
	V_{gc}	171.71V∟125.21°
Line impedance	Z_{ga}, Z_{gb}, Z_{gc}	2mH, 0.628Ω
Neutral impedance	Z_{gn}	100uH, 0.03Ω
Filter inductor	L_a, L_b, L_c	2mH, 0.03Ω
	L_n	0.67mH, 0.03Ω
Filter capacitor	C_a, C_b, C_c	5μF
DC-bus	V_{DC}	700V
Switching frequency	f_{sw}	16kHz

Table. (1).

VI. Conclusion:

In this paper, the detailed control of grid-interfacing inverters supporting negative-sequence voltage correction has been presented from basic principle. Based on the voltage unbalance factor and the system's capacity, the inverter absorbs a small amount of negative-sequence current from the grid, thereby correcting the negative sequence voltage. It has been shown that a grid-interfacing inverter, in addition to its normal operation, can help to decrease the negative-sequence voltage at the PoC. By using many of these modules, a substantial improvement is possible. Furthermore, the improved multi-variable filter can filter out positive- and negative-sequence components accurately in case of unbalanced/distorted situations in the stationary frame. The functionality and control scheme are verified by simulation results are shown.

VII. References:

[1]   Annette von Jouanne and Basudeb (Ben) Banerjee, "Assessment of voltage unbalance," *IEEE Trans. Power Del.*, vol. 16, no. 4, pp.782-790, Oct. 2001.
[2]   Hideaki Fujita, and H. Akagi, "Voltage-regulation performance of a shunt active filter intended for installation on a power distribution system," *IEEE Trans. Power Electron.*, vol 22, no. 3, pp. 1046-1053, May 2007.
[3]   Kuang Li, Jinjun Liu, and Zhaoan Wang, and Biao Wei, "Strategies and operating point optimization of STATCOM control for voltage unbalance mitigation in three-phase three-wire systems," *IEEE Trans. Power Del.*, vol. 22, no. 1, pp. 413-422, Jan. 2007.
[4]   Kalyan K. Sen, "SSSC-static synchronous series compensator theory, modeling, and application," *IEEE Trans. Power Del.*, vol. 13,

[5] Vijay B. Bhavaraju and Prasad N. Enjeti, "An active line conditioner to balance voltages in a three-phase system," *IEEE Trans. Ind. Applicat.*, vol. 32, no. 2, pp. 287-292, Mar./Apr. 1996

[6] Hideaki Fujita, H. Akagi, "The unified power quality conditioner: the integration of series- and shunt-active filters," *IEEE Trans. Power Electron.*, vol.13, no. 2, pp. 315-322, Mar. 1998.

[7] Dusan Graovac, V. A. Katic, and A. Rufer, " Power quality problems compensation with universal power quality conditioning system," *IEEE Trans. Power Del.* , vol. 22, no. 2, pp. 968-976, Apr. 2007.

[8] Koen J. P. Macken, Koen Vanthournout, Jeroen Van den Keybus, Geert Deconinck, and Ronnie J. M. Belmans, "Distributed Control of Renewable Generation Units With Integrated Active Filter," *IEEE Trans. Power Electron.*, vol. 19, no. 5, pp. 1353-1360, Sep. 2004.

[9] G. Jos, B.-T. Ooi, D. McGillis, F. D. Galiana and R. Marceau, "The potential of distributed generation to provide ancillary services," in *Proc. IEEE Power Eng. Soc. Summer Meeting*, Seattle, WA, July, 2000.

[10] P. M. Andersson, *Analysis of faulted power systems*, New York: IEEE Press, 1995.

[11] Fei Wang, Jorge L. Duate, Marcel A. M. Hendrix, "Weighting function integrated in grid-interfacing converters for unbalanced voltage correction," in *Proc. International Conf. on Renewable Energy and Power Quality (ICREPQ)*, Santander, Spain, 2008.

[12] M. C. Benhabib and S. Saadate, "A new robust experimentally validated phase locked loop for power electroni control," *European Power Electronics and Drives Journal*, vol. 15, no. 3, pp. 36-48, Aug. 2005.

[13] R. Teodorescu, F. Blaabjerg, M. Liserre and P.C. Loh, "Proportional-resonant controllers and filters for grid-connected voltage-source converters," *IEE Proc.-Electr. Power Appl.*, Vol. 153, No. 5, pp. 750-762, September 2006.

VIII. Manuscript of Authors:

K.Jayakumar[1] has received his B.Tech degree in EEE from Gokul Institute of Technology & Sciences, Bobbili in 2009. At present he is pursuing his M.Tech degree with the specialization of power electronics from Sri Vasavi Engineering College, Tadepalligudem, A.P. His areas of interest are power electronics & drives.

N.Sriharish[2] has received the Bachelor of Engineering degree in Electrical & Electronics Engineering from Anna University, in 2005 and Master's degree from JNTU Kakinada in 2010. Currently, he is an Assistant Professor at Sri Vasavi Engineering College, Tadepalligudem, A.P. His interests are in power system, power electronics and FACTS.

Ch.Rambabu[3] has received the Bachelor of Engineering degree in Electrical & Electronics Engineering from Madras University, in 2000 and Master's degree from JNTU Anantapur in 2005. He is a research student of JNTU Kakinada. Currently, he is a Professor & HOD at Sri Vasavi Engineering College, Tadepalligudem, A.P. His interests are in power system control and FACTS.